

Received June 28, 2018, accepted August 5, 2018, date of publication August 31, 2018, date of current version September 21, 2018.

Digital Object Identifier 10.1109/ACCESS.2018.2867574

Robust Actuator Fault Detection and Diagnosis for a Quadrotor UAV With External Disturbances

YUJIANG ZHONG^{ID1,2}, YOUMIN ZHANG^{ID2}, (Senior Member, IEEE), WEI ZHANG¹, JUNYI ZUO¹, AND HAO ZHAN¹

¹School of Aeronautics, Northwestern Polytechnical University, Xi'an 710072, China

²Department of Mechanical, Industrial & Aerospace Engineering, Concordia University, Montreal, QC H3G 1M8, Canada

Corresponding author: Wei Zhang (weizhangxian@nwpu.edu.cn)

This work was supported in part by the National Natural Science Foundation of China under Grant 11472222, Grant 61573282, and Grant 61473227 and in part by the Natural Sciences and Engineering Research Council of Canada.

ABSTRACT This paper presents a robust actuator fault detection and diagnosis (FDD) scheme for a quadrotor UAV (QUAV) in the presence of external disturbances. First, the dynamic model of a QUAV taking into account actuator faults and external disturbances is constructed. Then, treating the actuator faults and external disturbances as augmented system states, an adaptive augmented state Kalman filter (AASKF), is developed without the need of make the assumption that the exact stochastic information of actuator faults and external disturbances are available. Next, in order to reduce the computational load of AASKF, an adaptive three-stage Kalman filter (AThSKF) is proposed by decoupling the AASKF into three sub-filters. The AThSKF-based FDD scheme can not only detect and isolate actuator faults but also estimate the magnitudes even if the QUAV suffers from the external disturbances. Finally, the performance of the FDD scheme is evaluated under different fault scenarios, and simulation results demonstrate the effectiveness of the proposed method.

INDEX TERMS Actuators, fault detection, fault diagnosis, adaptive filters, unmanned aerial vehicles.

I. INTRODUCTION

In recent years, the quadrotor UAV (QUAV) has received a great deal of attention as a special kind of UAVs. Owing to the unique capabilities of vertical takeoff and landing and hovering, this vehicle has been widely employed in many areas, for example, security patrol [1], forest fire surveillance [2], inspection of power lines [3], and various military applications [4]. Compared with conventional aircraft, the advantages of QUAV have contributed to its unprecedented growth in aviation community. The satisfactory performance, safety and reliability are fundamental requirements in the QUAV system to complete the flight mission successfully. However, some specific applications will take the QUAV into hostile environments, such as strong wind. Furthermore, as a consumable hardware device, a QUAV is often equipped with low-cost and poor-quality components. These situations may lead to system failures and decrease the safety of QUAV [5]. The occurrence of faults in the QUAV system can not only easily damage the QUAV itself, but also seriously threaten the safety of human and environment. Especially, when flying over urban areas, the crash of QUAV will causes enormous casualty and property loss [6]. Early and reliable

detection and diagnosis of various faults in the QUAV system are crucial to avoiding the tragedy of wreck. The accurate fault information will be conducive to taking remedial actions quickly to guarantee the safety operation of QUAV. Therefore, in order to improve the safety, reliability and survivability of QUAV [7], it is highly desirable to design a QUAV system with the capability to detect and diagnosis faults.

As the link between control commands and physical actions, actuators play a crucial role in the QUAV system. During normal operation, the physical actions can be carried out as expected [8]. When faults occur in actuators, the control commands will fail to be conducted exactly, and the QUAV will operate in an unanticipated manner. More seriously, actuator faults may result in a crash of QUAV. Due to unexpected damage and component degradation, actuators are more prone to various faults. It is reported that most of flight accidents are induced by actuator faults. To deal with actuator faults and enhance the safety of QUAV, some notable fault detection and diagnosis (FDD) schemes have been proposed in the last decade. Amoozgar *et al.* [9] proposed a two-stage Kalman filter to detect, isolate and estimate

possible faults in each motor, and this FDD method was evaluated through experimental application in a real-time indoor QUAV testbed. Avram *et al.* [10] presented a fault detection, isolation and accommodation scheme for actuator faults by means of nonlinear adaptive estimation technique. A fault detection estimator and a set of fault isolation estimators were developed in this fault diagnosis architecture, and adaptive thresholds were designed to enhance the robustness of the diagnostic algorithm. Cen *et al.* [11] developed an adaptive Thau observer to estimate system states, and built a bank of offset residuals to detect and isolate actuator faults, as well as estimate the fault parameters. This FDD scheme could not only detect and isolate failed actuators, but also estimate the magnitude of faults. By integrating parity space method with recursive least squares algorithm, an FDD strategy for QUAV was introduced in [12], in which a residual was generated by the parity space method for actuator faults detection and the recursive least squares algorithm was used to estimate fault severities. In [13], a double-granularity FDD scheme was proposed based on a hybrid model of QUAV, which consists of a prior model and a set of non-parametric models. On the basis of prior model, a coarse-granularity-level FDD was implemented to isolate the faulty channel. Based on the non-parameter models, a fine-granularity-level FDD was built to isolate the specific variable in the faulty channel.

Although many effective actuator FDD methodologies for QUAV have been presented and validated on experimental platforms, there still exist some open issues to be solved. One major problem is detection and diagnosis of actuator faults when the QUAV is under influence of external disturbances. Generally, disturbances can be classified into internal disturbances (such as noises) and external disturbances (such as winds) [14], [15]. With respect to internal disturbances, some research has taken into account the impact on the performance of fault diagnosis [16]–[18]. However, little attention has been paid to the external disturbances. In practice, the QUAV system is inevitably affected by the external disturbances during the real flight, which can seriously degrade the performance of FDD schemes. What's worse, the small size and light weight of QUAV make the vehicle more sensitive to external disturbances. For example, a strong wind may destroy the stability of the QUAV system. Since the actuator faults and the external disturbances affect the QUAV system in the same manner, it is more difficult to distinguish them. In this case, the aforementioned FDD methods may not work perfectly or even diverge. It should be noted that the robust control of QUAV have been extensively studied (see for example [19]–[23]), but few results on actuator FDD techniques against external disturbances for QUAV have been reported in the literature. For the conventional aircraft, Lu [24] did a series of studies on actuator faults or sensor faults in the presence of the external disturbances. For a network of unmanned vehicles, Meskin *et al.* [25] designed a hybrid fault detection and isolation strategy to cope with actuator faults and large environment disturbances. Due to

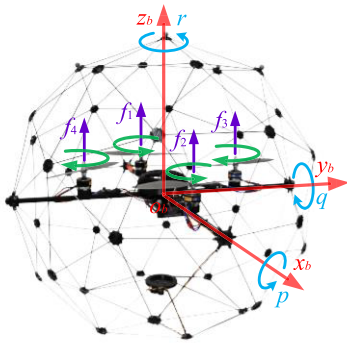
the differences in models, these methods are not adoptable for QUAV systems. In addition, the previous FDD schemes are designed on the assumption that the dynamical model of actuator faults and external disturbances are accurate. However, the assumption is invalid in the practical applications. This makes it more challenging to design a reliable and accurate FDD scheme.

Motivated by the aforementioned challenges, a robust actuator FDD scheme for QUAV subjected to external disturbances is proposed in this paper. To facilitate the design of the FDD scheme, a dynamic model of QUAV, which considering actuator faults and external disturbances, is firstly presented. Then, an adaptive augmented state Kalman filter is developed to detect and estimate the actuator faults. However, the computational cost of this filter is expensive due to the increased dimension of system state. To tackle the problem, an adaptive three-stage Kalman filter is further proposed, which can significantly reduce the computational cost and effectively distinguish actuator faults and external disturbances. The main contributions of this paper include: 1) the problem of actuator FDD for QUAV in the presence of internal disturbances and external disturbances is successfully solved; 2) The proposed FDD scheme gets rid of the assumption that exact stochastic information of actuator faults and external disturbances is available. Even when the dynamic models of actuator faults and external disturbances are incomplete, the FDD scheme can give a satisfactory estimation of system states and actuator faults; 3) By using a forgetting technique, an adaptive three-stage Kalman filter is developed, which can be used not only in the actuator FDD for QUAV, but also in other applications, e.g., fault-tolerant control.

The structure of this paper is organized as follows. The dynamic model of QUAV, considering actuator faults and external disturbances, is described in Section II. The detailed design procedure of the robust FDD scheme is presented in Section III. Simulation results of the FDD scheme are given in Section IV. Finally, some conclusions are summarized in Section V.

II. PROBLEM FORMULATION

As illustrated in Fig. 1, the mechanical structure of QUAV is relatively simple. It consists of four independent controlled rotors mounted on a rigid cross frame. The thrusts and torques acting on the QUAV are generated by two pairs of identical fixed-pitched propellers. To balance the torques, one pair of propellers (1 and 2) rotate in clockwise direction while the other pair of propellers (3 and 4) rotate in counter-clockwise direction [26]. The movements of QUAV are achieved by varying the speeds of these independent rotors. The pitch or roll motion is produced by conversely changing the speeds of diametrically opposite rotors. The yaw motion is generated by mismatching the speed balance in clockwise and counter-clockwise rotors. Simultaneous adjusting the speeds of these rotors will make the vertical motion.

**FIGURE 1.** Schematic representation of a quadrotor UAV.

A. DYNAMIC MODEL OF QUAV WITH EXTERNAL DISTURBANCES

QUAV is an under-actuated nonlinear system because this vehicle has six degrees of freedom with solely four control inputs [1]. The dynamics of QUAV have been studied in some literature. As described in [27], assuming small angular velocities, the dynamic model of QUAV with external disturbances can be represented as follows.

$$\begin{cases} \ddot{x} = (\cos\phi\sin\theta\cos\psi + \sin\phi\sin\psi)\frac{u_z}{m} + d_1 \\ \ddot{y} = (\cos\phi\sin\theta\sin\psi - \sin\phi\cos\psi)\frac{u_z}{m} + d_1 \\ \ddot{z} = (\cos\phi\cos\theta)\frac{u_z}{m} - g + d_1 \\ \ddot{\phi} = \frac{I_y - I_z}{I_x}\dot{\theta}\dot{\phi} - \frac{I_r}{I_x}\dot{\theta}\Omega_r + \frac{u_\phi}{I_x} + d_2 \\ \ddot{\theta} = \frac{I_z - I_x}{I_y}\dot{\phi}\dot{\theta} - \frac{I_r}{I_y}\dot{\phi}\Omega_r + \frac{u_\theta}{I_y} + d_3 \\ \ddot{\psi} = \frac{I_x - I_y}{I_z}\dot{\phi}\dot{\theta} + \frac{u_\psi}{I_z} + d_4 \end{cases} \quad (1)$$

The total lift (u_z) and applied torques (u_ϕ , u_θ , u_ψ) have the following relationship with thrusts.

$$\begin{bmatrix} u_z \\ u_\phi \\ u_\theta \\ u_\psi \end{bmatrix} = \begin{bmatrix} 1 & 1 & 1 & 1 \\ l & -l & 0 & 0 \\ 0 & 0 & l & -l \\ K_\psi & K_\psi & -K_\psi & -K_\psi \end{bmatrix} \begin{bmatrix} f_1 \\ f_2 \\ f_3 \\ f_4 \end{bmatrix} \quad (2)$$

In addition, the thrust f_i generated by i th propeller is related to pulse width modulation (PWM) input of i th motor, which can be modeled as

$$f_i = K_m \frac{\omega_m}{s + \omega_m} u_i \approx K_m u_i \quad (3)$$

Remark 1: Because the time constant of motor is much smaller than that of a QUAV, the approximation in (3) is reasonable. The above parameters, in (1), (2), (3), are illustrated in Table 1 to help readers better understand the dynamic model of QUAV.

To facilitate the design of FDD scheme, a simplified linear model is more preferable than the nonlinear model (1). To this end, the following assumption is considered.

Assumption 1: The QUAV is assumed to be close to the hovering condition, so that $u_z \approx mg$ in the vertical direction.

TABLE 1. Nomenclature.

Parameter	Definition
x, y, z	coordinates of QUAV in the inertial frame
ϕ, θ, ψ	roll, pitch, yaw angles of QUAV
m	mass of QUAV
g	acceleration of gravity
I_x	moment of inertia along x axis of the body-fixed frame
I_y	moment of inertia along y axis of the body-fixed frame
I_z	moment of inertia along z axis of the body-fixed frame
I_r	moment of inertia along the propeller axis
u_z	total lift force
u_ϕ	moment of roll
u_θ	moment of pitch
u_ψ	moment of yaw
f_i	thrust generated by i th propeller
l	distance between the center of QUAV and the rotor axis
K_ψ	thrust-to-moment scaling factor
K_m	positive gain of actuator
ω_m	motor bandwidth
u_i	PWM input to the i th motor
d_1, d_2, d_3, d_4	external disturbances

It is also assumed that the roll motion and pitch motion are so slight that $\sin\phi \approx \phi$ and $\sin\theta \approx \theta$, and no yaw motion ($\psi = 0$) is generated throughout the flight.

According to the assumption 1, the dynamic model of QUAV (1) can be linearized as

$$\begin{cases} \ddot{x} = \theta g + d_1 \\ \ddot{y} = -\phi g + d_1 \\ \ddot{z} = \frac{u_z}{m} - g + d_1 \\ \ddot{\phi} = \frac{u_\phi}{I_x} + d_2 \\ \ddot{\theta} = \frac{u_\theta}{I_y} + d_3 \\ \ddot{\psi} = \frac{u_\psi}{I_z} + d_4 \end{cases} \quad (4)$$

Define $x = [x \ \dot{x} \ y \ \dot{y} \ z \ \dot{z} \ \phi \ \dot{\phi} \ \theta \ \dot{\theta} \ \psi \ \dot{\psi}]^T \in \mathbb{R}^n$ as the system state vector, $u = [u_1 \ u_2 \ u_3 \ u_4]^T \in \mathbb{R}^p$ as the control input vector, $d = [d_1 \ d_2 \ d_3 \ d_4]^T \in \mathbb{R}^q$ as the external disturbance vector, $y = [x \ y \ z \ \phi \ \theta \ \psi]^T \in \mathbb{R}^m$ as the system output vector, the state-space representation of the dynamic model (4) can be expressed as

$$\begin{cases} \dot{x} = Ax + Bu + Fd + Gg \\ y = Cx \end{cases} \quad (5)$$

where

$$A = \begin{bmatrix} 0 & 1 & 0 & 0 & 0 & 0 & 0 & 0 & 0 & 0 & 0 & 0 \\ 0 & 0 & 0 & 0 & 0 & 0 & 0 & 0 & g & 0 & 0 & 0 \\ 0 & 0 & 0 & 1 & 0 & 0 & 0 & 0 & 0 & 0 & 0 & 0 \\ 0 & 0 & 0 & 0 & 0 & 0 & -g & 0 & 0 & 0 & 0 & 0 \\ 0 & 0 & 0 & 0 & 0 & 1 & 0 & 0 & 0 & 0 & 0 & 0 \\ 0 & 0 & 0 & 0 & 0 & 0 & 0 & 0 & 0 & 0 & 0 & 0 \\ 0 & 0 & 0 & 0 & 0 & 0 & 0 & 0 & 0 & 0 & 0 & 0 \\ 0 & 0 & 0 & 0 & 0 & 0 & 0 & 1 & 0 & 0 & 0 & 0 \\ 0 & 0 & 0 & 0 & 0 & 0 & 0 & 0 & 0 & 0 & 0 & 0 \\ 0 & 0 & 0 & 0 & 0 & 0 & 0 & 0 & 0 & 1 & 0 & 0 \\ 0 & 0 & 0 & 0 & 0 & 0 & 0 & 0 & 0 & 0 & 0 & 0 \\ 0 & 0 & 0 & 0 & 0 & 0 & 0 & 0 & 0 & 0 & 0 & 1 \end{bmatrix}$$

$$B = \begin{bmatrix} 0 & 0 & 0 & 0 \\ 0 & 0 & 0 & 0 \\ 0 & 0 & 0 & 0 \\ 0 & 0 & 0 & 0 \\ 0 & 0 & 0 & 0 \\ \frac{K_m}{m} & \frac{K_m}{m} & \frac{K_m}{m} & \frac{K_m}{m} \\ \frac{m}{0} & \frac{m}{0} & \frac{m}{0} & \frac{m}{0} \\ \frac{K_m l}{I_x} & -\frac{K_m l}{I_x} & 0 & 0 \\ 0 & 0 & 0 & 0 \\ 0 & 0 & \frac{K_m l}{I_y} & -\frac{K_m l}{I_y} \\ 0 & 0 & 0 & 0 \\ \frac{K_m K_\psi}{I_z} & \frac{K_m K_\psi}{I_z} & -\frac{K_m K_\psi}{I_z} & -\frac{K_m K_\psi}{I_z} \end{bmatrix}$$

$$C = \begin{bmatrix} 1 & 0 & 0 & 0 & 0 & 0 & 0 & 0 & 0 & 0 & 0 \\ 0 & 0 & 1 & 0 & 0 & 0 & 0 & 0 & 0 & 0 & 0 \\ 0 & 0 & 0 & 0 & 1 & 0 & 0 & 0 & 0 & 0 & 0 \\ 0 & 0 & 0 & 0 & 0 & 0 & 1 & 0 & 0 & 0 & 0 \\ 0 & 0 & 0 & 0 & 0 & 0 & 0 & 0 & 1 & 0 & 0 \\ 0 & 0 & 0 & 0 & 0 & 0 & 0 & 0 & 0 & 0 & 1 \end{bmatrix}$$

$$G = [0 \ 0 \ 0 \ 0 \ 0 \ -1 \ 0 \ 0 \ 0 \ 0 \ 0]^T$$

$$F = \begin{bmatrix} 0 & 1 & 0 & 1 & 0 & 1 & 0 & 0 & 0 & 0 & 0 \\ 0 & 0 & 0 & 0 & 0 & 0 & 0 & 1 & 0 & 0 & 0 \\ 0 & 0 & 0 & 0 & 0 & 0 & 0 & 0 & 0 & 1 & 0 \\ 0 & 0 & 0 & 0 & 0 & 0 & 0 & 0 & 0 & 0 & 1 \end{bmatrix}^T$$

B. FORMULATION OF ACTUATOR FAULTS

The actuators of QUAV are composed by four identical brushless motors and fixed-pitched propellers, as depicted in Fig.1. Due to the unexpected damage to these propellers or motors, the actuators may fail to operate as expected, which significantly decreases the reliability and safety of QUAV. The actuator faults considered in this paper refer to partial loss of control effectiveness, which is recognized as one of most common actuator faults [28]. Let $\gamma_i, i = 1, \dots, p$ denotes the loss of control effectiveness factor, when fault occurs in the i th actuator, the i th control input is formulated as

$$u_i^f = (1 - \gamma_i)u_i, \quad 0 \leq \gamma_i \leq \bar{\gamma}_i \leq 1 \quad (6)$$

where $\bar{\gamma}_i$ denotes the known upper bound that keeps the QUAV controllable. If $\gamma_i > \bar{\gamma}_i$, then the QUAV will become uncontrollable and may crash into the ground. $\gamma_i = 0$ indicates that the i th actuator works normally. $\gamma_i > 0$ represents that there is a loss of control effectiveness in the i th actuator. In an extreme case, $\gamma_i = \bar{\gamma}_i = 1$ means that the i th actuator breaks down completely.

By substituting (6) into (5), the dynamic model of QUAV considering actuator faults and external disturbances can be written as

$$\dot{x} = Ax + B(I - \Gamma)u + Fd + Gg \quad (7)$$

where

$$\Gamma = \begin{bmatrix} \gamma_1 & 0 & \cdots & 0 \\ 0 & \gamma_2 & \cdots & 0 \\ \vdots & \vdots & \ddots & 0 \\ 0 & 0 & \cdots & \gamma_p \end{bmatrix}$$

or in other form as

$$\dot{x} = Ax + Bu + E\gamma + Fd + Gg \quad (8)$$

where $E = -BU$ and

$$U = \begin{bmatrix} u_1 & 0 & \cdots & 0 \\ 0 & u_2 & \cdots & 0 \\ \vdots & \vdots & \ddots & 0 \\ 0 & 0 & \cdots & u_p \end{bmatrix}, \quad \gamma = \begin{bmatrix} \gamma_1 \\ \gamma_2 \\ \vdots \\ \gamma_p \end{bmatrix}$$

C. DISCRETE-TIME DYNAMIC MODEL OF QUAV CONSIDERING EXTERNAL DISTURBANCES AND ACTUATOR FAULTS

Since the proposed FDD scheme is designed based on a discrete filter, it is necessary to discretize the dynamic model (8). By utilizing zero-order hold with sampling at 50Hz, a discrete-time dynamic model of QUAV subject to actuator faults and external disturbances is represented as

$$\begin{cases} x_{k+1} = A_k x_k + B_k u_k + E_k \gamma_k + F_k d_k + G_k g + \omega_k^x \\ y_k = C_k x_k + v_k \end{cases} \quad (9)$$

where ω_k^x and v_k denote uncorrelated zero-mean white Gaussian noise sequences with covariances Q_k^x and R_k , respectively.

Remark 2: It should be noted that process noise ω_k and measurement noise v_k describe the system modeling error and sensor measurement noise, respectively. These noises can be regarded as internal disturbances of the QUAV system. Thus, the dynamic model (9) considers not only external disturbances but also internal disturbances.

In general, the dynamics of actuator faults and external disturbances are unknown, but we can model them as stochastic processes.

$$\gamma_{k+1} = \gamma_k + w_k^\gamma \quad (10)$$

$$d_{k+1} = d_k + w_k^d \quad (11)$$

where w_k^γ and w_k^d represent zero-mean white noise sequences. Furthermore, the noise sequences $\omega_k^x, v_k, w_k^\gamma$ and w_k^d satisfy the following conditions.

$$E \left\{ \begin{bmatrix} \omega_k^x \\ \omega_k^\gamma \\ \omega_k^d \\ v_k \end{bmatrix} \begin{bmatrix} \omega_l^x \\ \omega_l^\gamma \\ \omega_l^d \\ v_l \end{bmatrix}^T \right\} = \begin{bmatrix} Q_k^x & Q_k^{xy} & Q_k^{xd} & 0 \\ Q_k^{yx} & Q_k^\gamma & Q_k^{yd} & 0 \\ Q_k^{dx} & Q_k^{dy} & Q_k^d & 0 \\ 0 & 0 & 0 & R_k \end{bmatrix} \delta_{kl} \quad (12)$$

where $E\{\cdot\}$ is the expectation function, and δ_{kl} is the Kronecker delta.

III. FAULT DETECTION AND DIAGNOSIS SCHEME

The mathematical model (9) describes the dynamics of QUAV subjected to actuator faults and external disturbances. From (9), it is easy to know these two exogenous signals affect the QUAV system in the same way, thus it is an enormous challenge to distinguish them. To tackle the problem, an adaptive three-stage Kalman filter (AThSKF) is proposed in this section.

A. ADAPTIVE AUGMENTED STATE KALMAN FILTER

Consider the dynamic model (9), augmented state technique [29] is a useful tool for estimating the system state and unknown input simultaneously. Therefore, treating actuator faults γ_k and external disturbances d_k as the augmented system states, the dynamic model (9), (10) and (11) can be reformulated as

$$\begin{cases} x_{k+1}^a = A_k^a x_k^a + B_k^a u_k + G_k g + w_k^a \\ y_k = C_k^a x_k^a + v_k \end{cases} \quad (13)$$

where

$$\begin{aligned} A_k^a &= \begin{bmatrix} A_k & E_k & F_k \\ 0 & I & 0 \\ 0 & 0 & I \end{bmatrix}, \quad x_{(\cdot)}^a = \begin{bmatrix} x_{(\cdot)} \\ \gamma_{(\cdot)} \\ d_{(\cdot)} \end{bmatrix}, \quad B_k^a = \begin{bmatrix} B_k \\ 0 \\ 0 \end{bmatrix} \\ w_k^a &= \begin{bmatrix} w_k^x \\ w_k^\gamma \\ w_k^d \end{bmatrix}, \quad C_k^a = [C_k \quad 0 \quad 0] \end{aligned}$$

Remark 3: The system states of the normal dynamic model (9) and the augmented dynamic model (13) are observable. The observability of these systems can be analysed by observability theorem. It can be proved that the observability matrices ($O = [C_k^T \ A_k^T \ C_k^T \ \cdots \ (A_k^T)^{n-1} \ C_k^T]$ and $O_a = [(C_k^a)^T \ (A_k^a)^T \ (C_k^a)^T \ \cdots \ \{(C_k^a)^T\}^{n+p+q-1} \ (C_k^a)^T]$) are of full rank.

Remark 4: Because the term $G_k g$ is a constant matrix, it has no effect on the design of FDD strategy. For the sake of convenience, this term will be dropped in the rest of the section.

When an accurate system model (9) and exact dynamic evolutions of actuator faults (10) and external disturbances (11) are available, the augmented state Kalman filter (ASKF) [30] could give an optimal solution to the above problem, which is described as

$$\hat{x}_{k|k-1}^a = A_{k-1}^a \hat{x}_{k-1|k-1}^a + B_{k-1}^a u_{k-1} \quad (14)$$

$$P_{k|k-1}^a = A_{k-1}^a P_{k-1|k-1}^a A_{k-1}^{aT} + Q_{k-1}^a \quad (15)$$

$$K_k^a = P_{k|k-1}^a C_k^{aT} (C_k^a P_{k|k-1}^a C_k^{aT} + R_k)^{-1} \quad (16)$$

$$\hat{x}_{k|k}^a = \hat{x}_{k|k-1}^a + K_k^a (y_k - C_k^a \hat{x}_{k|k-1}^a) \quad (17)$$

$$P_{k|k}^a = (I - K_k^a C_k^a) P_{k|k-1}^a \quad (18)$$

where

$$\begin{aligned} P_{(\cdot)}^a &= \begin{bmatrix} P_{(\cdot)}^x & P_{(\cdot)}^{xy} & P_{(\cdot)}^{xd} \\ P_{(\cdot)}^{yx} & P_{(\cdot)}^y & P_{(\cdot)}^{yd} \\ P_{(\cdot)}^{dx} & P_{(\cdot)}^{dy} & P_{(\cdot)}^d \end{bmatrix}, \quad K_k^a = \begin{bmatrix} K_k^x \\ K_k^\gamma \\ K_k^d \end{bmatrix} \\ Q_{(\cdot)}^a &= \begin{bmatrix} Q_{(\cdot)}^x & Q_{(\cdot)}^{xy} & Q_{(\cdot)}^{xd} \\ Q_{(\cdot)}^{yx} & Q_{(\cdot)}^y & Q_{(\cdot)}^{yd} \\ Q_{(\cdot)}^{dx} & Q_{(\cdot)}^{dy} & Q_{(\cdot)}^d \end{bmatrix} \end{aligned}$$

However, in practice, the statistical properties of unknown inputs (10) and (11) are not perfectly known or unavailable, so that the performance of the ASKF algorithm may be unsatisfactory or even diverge. Hence, it would be better if a robust augmented state Kalman filter could be designed to get a better estimation in this condition.

Innovation is an important quantity of the optimal filter, and can be employed to evaluate the filter performance. Consider the innovation of ASKF, which is defined as

$$\eta_k^a = y_k - C_k^a \hat{x}_{k|k-1}^a \quad (19)$$

Then, the theoretical innovation covariance of ASKF can be obtained as

$$\Xi_k^a = E[\eta_k^a \eta_k^{aT}] = C_k^a P_{k|k-1}^a C_k^{aT} + R_k \quad (20)$$

the real innovation covariance is computed as

$$\tilde{\Xi}_k^a = \frac{1}{M-1} \sum_{i=k-M+1}^k \eta_i \eta_i^T \quad (21)$$

and the innovation auto-covariance of ASKF is presented as

$$\begin{aligned} \Xi_{k+j,k}^a &= E[\eta_{k+j}^a \eta_k^{aT}] \\ &= C_{k+j}^a A_{k+j-1}^a [I - K_{k+j-1}^a C_{k+j-1}^a] \cdots A_{k+1}^a \\ &\quad \cdot [I - K_{k+1}^a C_{k+1}^a] A_k^a [P_{k|k-1}^a C_k^{aT} - K_k^a \Xi_k^a] \\ &\quad \forall j = 1, 2, 3, \dots \end{aligned} \quad (22)$$

If the dynamic model (13) is exactly known, ASKF is optimal in a minimum mean square error sense and $\Xi_k^a = \tilde{\Xi}_k^a$. Substituting optimal gain (16) into (22), $\Xi_{k+j,k}^a$ is identical to zero, which indicates that the innovation η_k^a is a white sequence when the optimal gain is used. However, due to modeling errors and unknown noise covariances, the real innovation covariance $\tilde{\Xi}_k^a$ is different from the theoretical one Ξ_k^a . Therefore, $\Xi_{k+j,k}^a$ may not anymore be identically zero. In this case, if a measure can be taken to make $\Xi_{k+j,k}^a = 0$, then ASKF is still optimal [31].

To solve the previous problem, a well-known technique is the application of forgetting factors, which enables the filter to eliminate the effect of old information. Inspired by [32], a forgetting factor λ_k^a is introduced into the time update equation (15) in the following form.

$$\tilde{P}_{k|k-1}^a = \lambda_k^a P_{k|k-1}^a = \lambda_k^a (A_{k-1}^a P_{k-1|k-1}^a A_{k-1}^{aT} + Q_{k-1}^a) \quad (23)$$

Theorem 1: An adaptive augmented state Kalman filter (AASKF) is given by (14)-(18) with a replacement (15)

by (23), and the forgetting factor λ_k^a is calculated by

$$\lambda_k^a = \max \left\{ 1, \frac{1}{m} \text{trace} \left[(\tilde{\Xi}_k^a - R_k) (C_k^a P_{k|k-1}^a C_k^{aT})^{-1} \right] \right\} \quad (24)$$

or

$$\lambda_k^a = \max \left\{ 1, \frac{\text{trace}(\tilde{\Xi}_k^a - R_k)}{\text{trace}(C_k^a P_{k|k-1}^a C_k^{aT})} \right\} \quad (25)$$

Proof: Define

$$S_k^a = P_{k|k-1}^a C_k^{aT} - K_k^a \Xi_k^a \quad (26)$$

If S_k^a is equal to zero matrix, it is obvious that $\Xi_{k+j,k}^a$ is also equivalent to zero. Substituting (16) into (26) gives

$$S_k^a = P_{k|k-1}^a C_k^{aT} [I - (C_k^a P_{k|k-1}^a C_k^{aT} + R_k)^{-1} \Xi_k^a] \quad (27)$$

Since $P_{k|k-1}^a$ is nonsingular and C_k^a is of full rank, $S_k^a = 0$ implies

$$(C_k^a P_{k|k-1}^a C_k^{aT} + R_k)^{-1} \Xi_k^a = I \quad (28)$$

When model errors and unknown noise covariances occur, Ξ_k^a is not identical to $\tilde{\Xi}_k^a$. Thus, S_k^a is not equivalent to zero. Substituting the real innovation covariance $\tilde{\Xi}_k^a$ and (23) into (28) generates

$$\lambda_k^a C_k^a P_{k|k-1}^a C_k^{aT} = \tilde{\Xi}_k^a - R_k \quad (29)$$

then

$$\lambda_k^a I = (\tilde{\Xi}_k^a - R_k) (C_k^a P_{k|k-1}^a C_k^{aT})^{-1} \quad (30)$$

Therefore, (24) can be obtained from (30). In order to avoid inversion manipulation, (25) can be computed by taking trace in both sides of (29).

Remark 5: When the model is accurately built, $\tilde{\Xi}_k^a = \Xi_k^a$. Substituting $\tilde{\Xi}_k^a = \Xi_k^a$ into (24) or (25), we have $\lambda_k^a = 1$, which implies that AASKF is reduced to ASKF in this case.

B. ADAPTIVE THREE-STAGE KALMAN FILTER

AASKF can give an optimal estimation even if the system model is incomplete. However, an inherent drawback of AASKF is that the computational cost increases dramatically with the growth of dimension of system state. When the dimension of augmented system state is comparable to that of original system state, the computational cost is acceptable [33]. Unfortunately, the computational requirement will become excessive when original system state is significantly increased in dimension. To overcome this problem, AASKF is decoupled into three parallel sub-filters in this section.

Theorem 2: An adaptive three-stage Kalman filter (AThSKF) is described by the following difference equations when the statistical information of unknown inputs are not perfect known.

$$\hat{x}_{k|k} = \bar{x}_{k|k} + V_k^{12} \bar{\gamma}_{k|k} + V_k^{13} \bar{d}_{k|k} \quad (31)$$

$$P_{k|k}^x = \bar{P}_{k|k}^x + V_k^{12} \bar{P}_{k|k}^y V_k^{12T} + V_k^{13} \bar{P}_{k|k}^d V_k^{13T} \quad (32)$$

$$\bar{\gamma}_{k|k} = \bar{\gamma}_{k|k} + V_k^{23} \bar{d}_{k|k} \quad (33)$$

$$P_{k|k}^y = \bar{P}_{k|k}^y + V_k^{23} \bar{P}_{k|k}^d V_k^{23T} \quad (34)$$

$$\hat{d}_{k|k} = \bar{d}_{k|k} \quad (35)$$

$$P_{k|k}^d = \bar{P}_{k|k}^d \quad (36)$$

The state sub-filter is

$$\bar{x}_{k|k-1} = A_{k-1} \bar{x}_{k-1|k-1} + B_{k-1} u_{k-1} + \bar{u}_{k-1}^1 \quad (37)$$

$$\bar{P}_{k|k-1}^x = \lambda_k^x (\bar{P}_{k-1|k-1}^x A_{k-1}^T + \bar{Q}_{k-1}^1) \quad (38)$$

$$\bar{K}_k^x = \bar{P}_{k|k-1}^x S_k^{1T} (S_k^1 \bar{P}_{k|k-1}^x S_k^{1T} + R_k)^{-1} \quad (39)$$

$$\bar{x}_{k|k} = \bar{x}_{k|k-1} + \bar{K}_k^x \eta_k^x \quad (40)$$

$$\bar{P}_{k|k}^x = (I - \bar{K}_k^x S_k^1) \bar{P}_{k|k-1}^x \quad (41)$$

where

$$\eta_k^x = y_k - S_k^1 \bar{x}_{k|k-1}$$

$$\tilde{\Xi}_k^x = \frac{1}{M-1} \sum_{i=k-M+1}^k \eta_i^x \eta_i^{xT}$$

$$\lambda_k^x = \max \left\{ 1, \frac{\text{trace}(\tilde{\Xi}_k^x - R_k)}{\text{trace}(S_k^1 \bar{P}_{k|k-1}^x S_k^{1T})} \right\}$$

The fault sub-filter is

$$\bar{\gamma}_{k|k-1} = \bar{\gamma}_{k-1|k-1} + \bar{u}_{k-1}^2 \quad (42)$$

$$\bar{P}_{k|k-1}^y = \lambda_k^y (\bar{P}_{k-1|k-1}^y + \bar{Q}_{k-1}^2) \quad (43)$$

$$\bar{K}_k^y = \bar{P}_{k|k-1}^y S_k^{2T} (S_k^2 \bar{P}_{k|k-1}^y S_k^{2T} + S_k^1 \bar{P}_{k|k-1}^x S_k^{1T} + R_k)^{-1} \quad (44)$$

$$\bar{\gamma}_{k|k} = \bar{\gamma}_{k|k-1} + \bar{K}_k^y \eta_k^y \quad (45)$$

$$\bar{P}_{k|k}^y = (I - \bar{K}_k^y S_k^2) \bar{P}_{k|k-1}^y \quad (46)$$

where

$$\eta_k^y = y_k - S_k^1 \bar{x}_{k|k-1} - S_k^2 \bar{\gamma}_{k|k-1}$$

$$\tilde{\Xi}_k^y = \frac{1}{M-1} \sum_{i=k-M+1}^k \eta_i^y \eta_i^{yT}$$

$$\lambda_k^y = \max \left\{ 1, \frac{\text{trace}(\tilde{\Xi}_k^y - S_k^1 \bar{P}_{k|k-1}^y S_k^{1T} - R_k)}{\text{trace}(S_k^2 \bar{P}_{k|k-1}^y S_k^{2T})} \right\}$$

The disturbance sub-filter is

$$\bar{d}_{k|k-1} = \bar{d}_{k-1|k-1} \quad (47)$$

$$\bar{P}_{k|k-1}^d = \lambda_k^d (\bar{P}_{k-1|k-1}^d + \bar{Q}_{k-1}^d) \quad (48)$$

$$\bar{K}_k^d = \bar{P}_{k|k-1}^d S_k^{3T} (S_k^3 \bar{P}_{k|k-1}^d S_k^{3T} + S_k^2 \bar{P}_{k|k-1}^y S_k^{2T} + S_k^1 \bar{P}_{k|k-1}^x S_k^{1T} + R_k)^{-1} \quad (49)$$

$$\bar{d}_{k|k} = \bar{d}_{k|k-1} + \bar{K}_k^d \eta_k^d \quad (50)$$

$$\bar{P}_{k|k}^d = (I - \bar{K}_k^d S_k^3) \bar{P}_{k|k-1}^d \quad (51)$$

where

$$\eta_k^d = y_k - S_k^1 \bar{x}_{k|k-1} - S_k^2 \bar{\gamma}_{k|k-1} - S_k^3 \bar{d}_{k|k-1}$$

$$\tilde{\Xi}_k^d = \frac{1}{M-1} \sum_{i=k-M+1}^k \eta_i^d \eta_i^{dT}$$

$$\lambda_k^d = \max \left\{ 1, \frac{\text{trace}(\tilde{\Xi}_k^d - S_k^3 \bar{P}_{k|k-1}^d S_k^{3T} - S_k^2 \bar{P}_{k|k-1}^y S_k^{2T} - S_k^1 \bar{P}_{k|k-1}^x S_k^{1T} - R_k)}{\text{trace}(S_k^3 \bar{P}_{k|k-1}^d S_k^{3T})} \right\}$$

with the following coupled equations

$$V_k^{12} = U_k^{12} - \bar{K}_k^x S_k^2 \quad (52)$$

$$V_k^{13} = U_k^{13} - V_k^{12} \bar{K}_k^\gamma S_k^3 - \bar{K}_k^x S_k^3 \quad (53)$$

$$V_k^{23} = U_k^{23} - \bar{K}_k^\gamma S_k^3 \quad (54)$$

$$S_k^1 = C_k \quad (55)$$

$$S_k^2 = C_k U_k^{12} \quad (56)$$

$$S_k^3 = C_k U_k^{13} \quad (57)$$

$$\begin{aligned} \bar{u}_{k-1}^1 &= (\bar{U}_k^{12} - U_k^{12}) \bar{y}_{k-1|k-1} + (\bar{U}_k^{13} - U_k^{13} \\ &\quad - U_k^{12}(\bar{U}_k^{23} - U_k^{23})) \bar{d}_{k-1|k-1} \end{aligned} \quad (58)$$

$$\bar{u}_{k-1}^2 = (\bar{U}_k^{23} - U_k^{23}) \bar{d}_{k-1|k-1} \quad (59)$$

$$\begin{aligned} \bar{Q}_{k-1}^1 &= Q_{k-1}^x + \bar{U}_k^{12} \bar{P}_{k-1|k-1}^\gamma \bar{U}_k^{12T} - U_k^{12} \bar{P}_{k|k-1}^\gamma U_k^{12T} \\ &\quad + \bar{U}_k^{13} \bar{P}_{k-1|k-1}^d \bar{U}_k^{13T} - U_k^{13} \bar{P}_{k|k-1}^d U_k^{13T} \end{aligned} \quad (60)$$

$$\begin{aligned} \bar{Q}_{k-1}^2 &= Q_{k-1}^\gamma + \bar{U}_k^{23} \bar{P}_{k-1|k-1}^d \bar{U}_k^{23T} - U_k^{23} \bar{P}_{k|k-1}^d U_k^{23T} \end{aligned} \quad (61)$$

$$\begin{aligned} U_k^{12} &= (\bar{U}_k^{12} \bar{P}_{k-1|k-1}^\gamma + \bar{U}_k^{13} \bar{P}_{k-1|k-1}^d \bar{U}_k^{23T} \\ &\quad - U_k^{13} \bar{P}_{k-1|k-1}^\gamma \bar{U}_k^{23T} + Q_{k-1}^{xy})(\bar{P}_{k|k-1}^\gamma)^{-1} \end{aligned} \quad (62)$$

$$U_k^{13} = (\bar{U}_k^{13} \bar{P}_{k-1|k-1}^d + Q_{k-1}^{xd})(\bar{P}_{k|k-1}^d)^{-1} \quad (63)$$

$$U_k^{23} = (\bar{U}_k^{23} \bar{P}_{k-1|k-1}^d + Q_{k-1}^{yd})(\bar{P}_{k|k-1}^d)^{-1} \quad (64)$$

$$\bar{U}_k^{12} = A_{k-1} V_{k-1}^{12} + E_{k-1} \quad (65)$$

$$\bar{U}_k^{13} = A_{k-1} V_{k-1}^{13} + E_{k-1} V_{k-1}^{23} + F_{k-1} \quad (66)$$

$$\bar{U}_k^{23} = V_{k-1}^{23} \quad (67)$$

Proof: To decouple the AASKF, the following three-stage U-V transformation [34] is applied.

$$T(U_k) = \begin{bmatrix} I & U_k^{12} & U_k^{13} \\ 0 & I & U_k^{23} \\ 0 & 0 & I \end{bmatrix}, \quad T(V_k) = \begin{bmatrix} I & V_k^{12} & V_k^{13} \\ 0 & I & V_k^{23} \\ 0 & 0 & I \end{bmatrix} \quad (68)$$

where $U_k^{(\cdot)}$ and $V_k^{(\cdot)}$ will be determined later.

Based on the transformation operation, the augmented system state and error covariance are represented as

$$\hat{x}_{k|k-1}^a = T(U_k) \bar{x}_{k|k-1}^a \quad (69)$$

$$\hat{x}_{k|k}^a = T(V_k) \bar{x}_{k|k}^a \quad (70)$$

$$P_{k|k-1}^a = T(U_k) \bar{P}_{k|k-1}^a T^T(U_k) \quad (71)$$

$$P_{k|k}^a = T(V_k) \bar{P}_{k|k}^a T^T(V_k) \quad (72)$$

$$K_k^a = T(V_k) \bar{K}_k^a \quad (73)$$

where

$$\bar{x}_{(\cdot)}^a = \begin{bmatrix} \bar{x}_{(\cdot)} \\ \bar{\gamma}_{(\cdot)} \\ \bar{d}_{(\cdot)} \end{bmatrix}, \quad \bar{P}_{(\cdot)}^a = \begin{bmatrix} \bar{P}_{(\cdot)}^x & 0 & 0 \\ 0 & \bar{P}_{(\cdot)}^\gamma & 0 \\ 0 & 0 & \bar{P}_{(\cdot)}^d \end{bmatrix}, \quad \bar{K}_{(\cdot)}^a = \begin{bmatrix} \bar{K}_{(\cdot)}^x \\ \bar{K}_{(\cdot)}^\gamma \\ \bar{K}_{(\cdot)}^d \end{bmatrix}$$

Using the inverse U-V transformation, (69)-(73) become in the following form.

$$\bar{x}_{k|k-1}^a = T^{-1}(U_k) \hat{x}_{k|k-1}^a \quad (74)$$

$$\bar{x}_{k|k}^a = T^{-1}(V_k) \hat{x}_{k|k}^a \quad (75)$$

$$\bar{P}_{k|k-1}^a = T^{-1}(U_k) P_{k|k-1}^a T^{-T}(U_k) \quad (76)$$

$$\bar{P}_{k|k}^a = T^{-1}(V_k) P_{k|k}^a T^{-T}(V_k) \quad (77)$$

$$\bar{K}_k^a = T^{-1}(V_k) K_k^a \quad (78)$$

where

$$T^{-1}(U_k) = \begin{bmatrix} I & -U_k^{12} & U_k^{12} U_k^{23} - U_k^{13} \\ 0 & I & -U_k^{23} \\ 0 & 0 & I \end{bmatrix}$$

$$T^{-1}(V_k) = \begin{bmatrix} I & -V_k^{12} & V_k^{12} V_k^{23} - V_k^{13} \\ 0 & I & -V_k^{23} \\ 0 & 0 & I \end{bmatrix}$$

According to (74) - (78), AASKF is transformed into

$$\bar{x}_{k|k-1}^a = T^{-1}(U_k)(A_{k-1}^a \hat{x}_{k-1|k-1}^a + B_{k-1}^a u_{k-1}) \quad (79)$$

$$\bar{x}_{k|k}^a = T^{-1}(V_k) [\hat{x}_{k|k-1}^a + K_k^a (y_k - C_k^a \hat{x}_{k|k-1}^a)] \quad (80)$$

$$\begin{aligned} \bar{P}_{k|k-1}^a &= T^{-1}(U_k) \lambda_k^a (A_{k-1}^a P_{k-1|k-1}^a A_{k-1}^{aT} \\ &\quad + Q_{k-1}^a) T^{-T}(U_k) \end{aligned} \quad (81)$$

$$\bar{P}_{k|k}^a = T^{-1}(V_k) (I - K_k^a C_k^a) P_{k|k-1}^a T^{-T}(V_k) \quad (82)$$

$$\bar{K}_k^a = T^{-1}(V_k) P_{k|k-1}^a C_k^{aT} (C_k^a P_{k|k-1}^a C_k^{aT} + R_k)^{-1} \quad (83)$$

Substituting (69) - (73) into (79) - (83), we have

$$\begin{aligned} \bar{x}_{k|k-1}^a &= T^{-1}(U_k) A_{k-1}^a T(V_{k-1}) \bar{x}_{k-1|k-1}^a \\ &\quad + T^{-1}(U_k) B_{k-1}^a u_{k-1} \end{aligned} \quad (84)$$

$$\begin{aligned} \bar{x}_{k|k}^a &= T^{-1}(V_k) T(U_k) \bar{x}_{k|k-1}^a + \bar{K}_k^a (y_k - C_k^a T(U_k) \bar{x}_{k|k-1}^a) \end{aligned} \quad (85)$$

$$\begin{aligned} \bar{P}_{k|k-1}^a &= T^{-1}(U_k) \lambda_k^a (A_{k-1}^a T(V_{k-1}) \bar{P}_{k-1|k-1}^a \\ &\quad + T^T(V_{k-1}) A_{k-1}^{aT} + Q_{k-1}^a) T^{-T}(U_k) \end{aligned} \quad (86)$$

$$\begin{aligned} \bar{P}_{k|k}^a &= (T^{-1}(V_k) T(U_k) - \bar{K}_k^a C_k^a T(U_k)) \bar{P}_{k|k-1}^a \\ &\quad \cdot T^T(U_k) T^{-T}(V_k) \end{aligned} \quad (87)$$

$$\begin{aligned} \bar{K}_k^a &= T^{-1}(V_k) T(U_k) \bar{P}_{k|k-1}^a T^T(U_k) C_k^{aT} (C_k^a T(U_k) \\ &\quad - \bar{P}_{k|k-1}^a T^T(U_k) C_k^{aT} + R_k)^{-1} \end{aligned} \quad (88)$$

Define

$$S_k = C_k^a T(U_k) = [S_k^1 \ S_k^2 \ S_k^3] \quad (89)$$

$$\bar{U}_k = A_{k-1}^a T(V_{k-1}) = \begin{bmatrix} A_{k-1} & \bar{U}_k^{12} & \bar{U}_k^{13} \\ 0 & I & \bar{U}_k^{23} \\ 0 & 0 & I \end{bmatrix} \quad (90)$$

From (89) and (90), (55) - (57) and (65) - (67) are obtained. (37), (42), (47), (58) and (59) are derived by expanding (84). From (30), we can know that λ_k^a is the following diagonal matrix.

$$\lambda_k^a = \begin{bmatrix} \lambda_k^x & 0 & 0 \\ 0 & \lambda_k^\gamma & 0 \\ 0 & 0 & \lambda_k^d \end{bmatrix} \quad (91)$$

Based on (86) and (91), we can obtain (38), (43), (48) and (60) - (64). The calculated process of λ_k^x , λ_k^γ and λ_k^d is similar

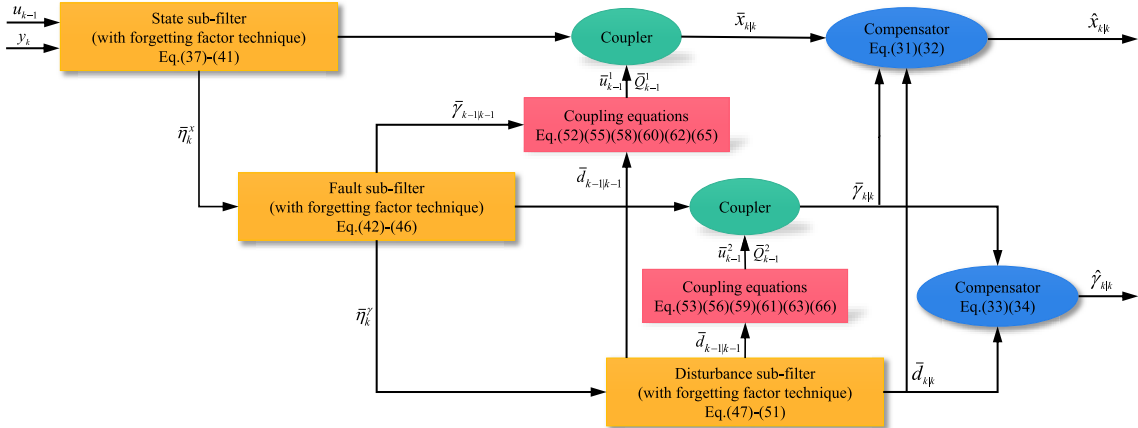


FIGURE 2. Framework of the AThSKF.

to that of λ_k^a . By developing (87), we can achieve (41), (46), (51) and (52)-(54). With reference to (88), we have (39), (44) and (49). Finally, referring to (70) and (72), (31)-(36) are obtained.

The framework of the AThSKF is shown in Fig. 2.

IV. SIMULATION RESULTS

In this section, some simulation results are presented to evaluate the performance of the proposed AThSKF-based FDD scheme. The dynamic model of QUAV used in this paper is Qball-X4, whose parameters are given in Table 2. In the simulation, the vehicle is commanded to hover at an altitude of 1 m, and actuator faults take place at a certain time. In order to adequately verify the effectiveness of the proposed FDD scheme, three different fault scenarios are considered. For the comparison of performance, the ASKF and ThSKF is also applied to show the advantages of the AThSKF. The covariance matrices used in the simulation are chosen as: $Q^x = \text{diag}\{10^{-6}I_{6 \times 6}, 10^{-12}I_{6 \times 6}\}$, $Q^y = 10^{-2}I_{4 \times 4}$, $Q^d = 10^{-3}I_{4 \times 4}$, $R = \text{diag}\{10^{-6}I_{3 \times 3}, 10^{-12}I_{3 \times 3}\}$. The initial values of the AThSKF are given by: $\bar{x}_0 = 0_{12 \times 1}$, $\bar{y}_0 = 0_{4 \times 1}$, $\bar{d}_0 = 0_{4 \times 1}$, $P_0^x = 10I_{12 \times 12}$, $P_0^y = 10I_{4 \times 4}$, $P_0^d = 10I_{4 \times 4}$. It should be noted that Q^x , Q^y and Q^d are used to generate the true system values. To demonstrate the robustness of the AThSKF, we assume that Q_k^x , Q_k^y and Q_k^d are not perfectly known and they are not equivalent to Q^x , Q^y and Q^d , respectively.

A. SCENARIO 1: SINGLE ACTUATOR FAULT WITHOUT EXTERNAL DISTURBANCES

In the first scenario, two consecutive partial losses of control effectiveness are injected in the second motor in the absence of external disturbances. First, the second motor is assumed to lose 20% of the normal control effectiveness at time $t = 20$ s, then the actuator fault becomes more serious and the magnitude changes from 20% to 45% at time $t = 40$ s. Under this fault condition, the simulation results are shown in Figs. 3, 4 and 5.

TABLE 2. System parameters of Qball-X4.

Parameter	Value	Unit
K_m	120	N
K_ψ	4	N·m
l	0.2	m
I_x	0.03	Kg·m ²
I_y	0.03	Kg·m ²
I_z	0.04	Kg·m ²
m	1.42	Kg
g	9.81	m/s ²

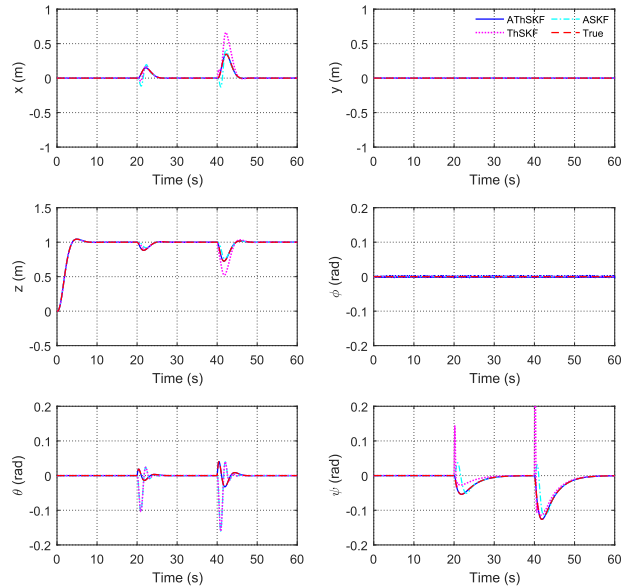


FIGURE 3. State estimation performance of ASKF, ThSKF and AThSKF in scenario 1.

The state estimates are shown in Fig. 3. It can be seen that the true and estimated state by using AThSKF are matched perfectly. Even though the system state changed significantly after the actuator fault occurs, the estimated value obtained by the AThSKF can track the true one. By contrast, the state estimation performance of ASKF and ThSKF are

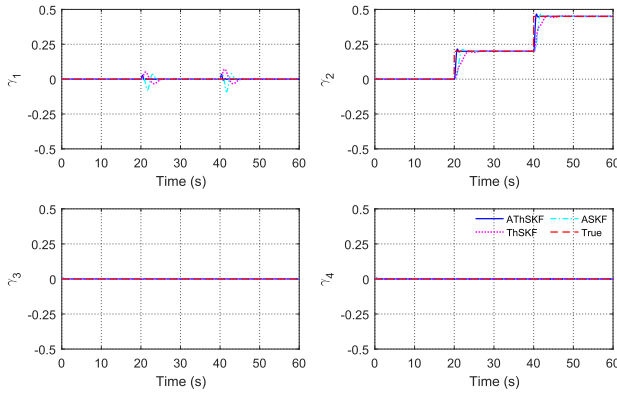


FIGURE 4. Fault estimation performance of ASKF, ThSKF and ATsKF in scenario 1.

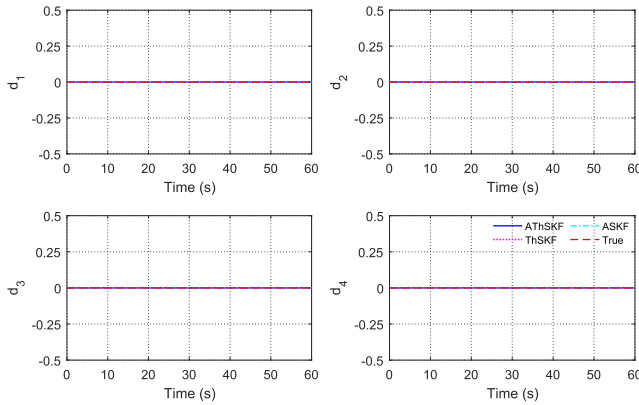


FIGURE 5. Disturbance estimation performance of ASKF, ThSKF and ATsKF in scenario 1.

unsatisfactory when the actuator abruptly fail to operate. As displayed in Fig.4, the proposed ATsKF can give a fast and accurate fault estimation. After fault injection in the second motor, the estimate of γ_2 converges rapidly to 0.2 at time $t = 21$ s and 0.45 at time $t = 41$ s, respectively. Meanwhile, the estimates of γ_1 , γ_3 and γ_4 still keep close to zero. Compared with the ASKF and ThSKF, ATsKF has faster convergence speed. Moreover, there are some false estimates in γ_1 by using ASKF and ThSKF. From Fig.5, it can be found that the estimates of external disturbances are zero all the time.

B. SCENARIO 2: SINGLE ACTUATOR FAULT WITH EXTERNAL DISTURBANCES

In the second scenario, it is assumed that the QUAV is affected by the external disturbances. To demonstrate the performance of the proposed FDD scheme, the external disturbances are simulated as wind gusts, which are more common and very difficult to handle in the practical applications. In the simulation, the wind gusts are generated by the Dryden model, the wind velocity V_w is set to 10 m/s, the sampling period T_s is selected as 0.02s, and the other parameters are as same as that in [35]. The generated disturbances d_k are displayed by red dashed lines in Fig. 8. With the influence

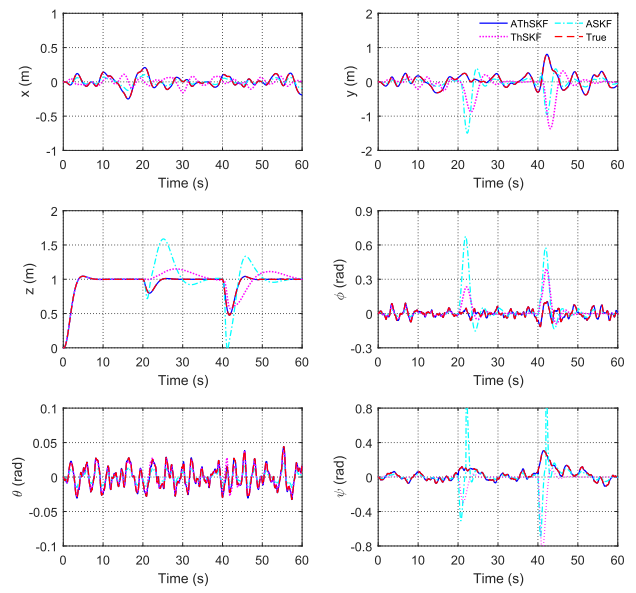


FIGURE 6. State estimation performance of ASKF, ThSKF and ATsKF in scenario 2.

of external disturbances, the 30% and 60% loss of control effectiveness are introduced into the third motor at $t = 20$ s and $t = 40$ s, respectively. The simulation results are shown in Figs. 6, 7 and 8.

As shown in Fig. 6, the state estimation performance of ATsKF is satisfactory, even in the presence of external disturbances. However, the estimation results obtained by the ASKF and ThSKF are affected by external disturbances. Both ASKF and ThSKF cannot track the true system state after the occurrence of actuator faults. In addition, the fault estimation performance of ASKF and ThSKF are deteriorated than that of ATsKF. As can be observed in Fig. 7, the proposed ATsKF can effectively detect and estimate the actuator faults within less than 1s. On the contrary, ASKF and ThSKF almost lost the capability for estimating the loss of control effectiveness factor. Fig. 8 presents the disturbance estimation performance of ASKF, ThSKF and ATsKF, it can be clearly seen that the disturbance estimation performance using ASKF and ThSKF are poor while ATsKF can still give an accurate disturbance estimation.

C. SCENARIO 3: SIMULTANEOUS ACTUATOR FAULTS WITH EXTERNAL DISTURBANCES

In the third scenario, simultaneous actuator faults with external disturbances are performed to demonstrate the advantages of the proposed ATsKF approach. The external disturbances are as same as that in scenario 2. It is assumed that the second and third motor simultaneously lose 30% of the normal control effectiveness at the same time $t = 20$ s, the another actuator fault takes place at $t = 40$ s with 45% loss of control effectiveness in the first motor. The simulation results are shown in Figs. 9, 10 and 11.

As can be seen in Fig. 9, the state estimation performance of ATsKF is more superior than that of ASKF and ThSKF.

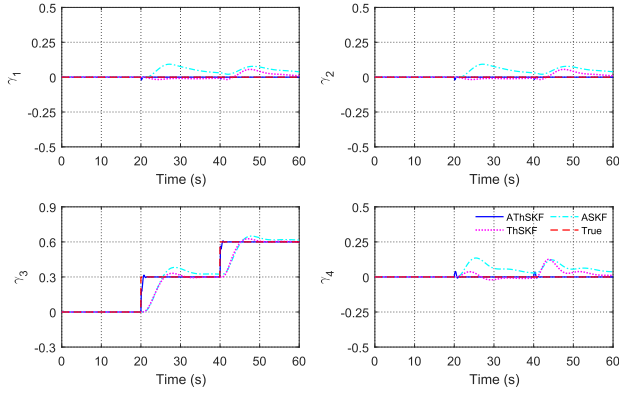


FIGURE 7. Fault estimation performance of ASKF, ThSKF and ATsKF in scenario 2.

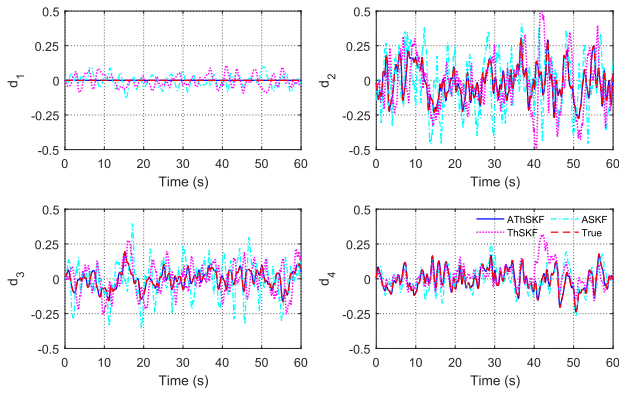


FIGURE 8. Disturbance estimation performance of ASKF, ThSKF and ATsKF in scenario 2.

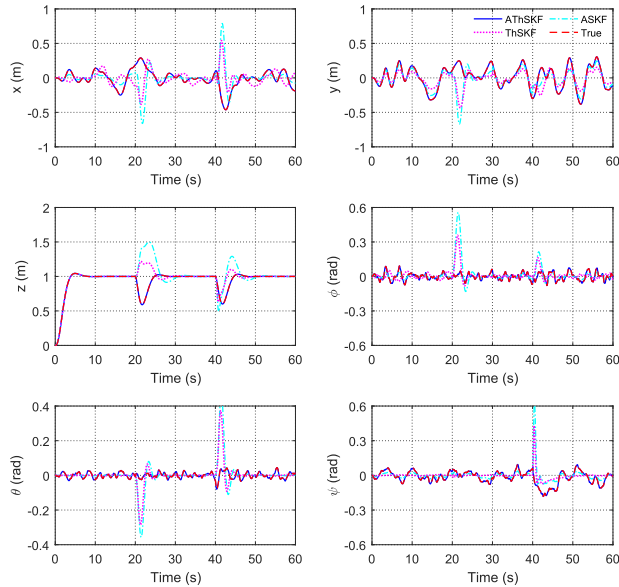


FIGURE 9. State estimation performance of ASKF, ThSKF and ATsKF in scenario 3.

The ATsKF still maintains satisfactory performance despite that two actuator faults occur simultaneously. Notice that the ASKF and ThSKF perform poorly when the faults are

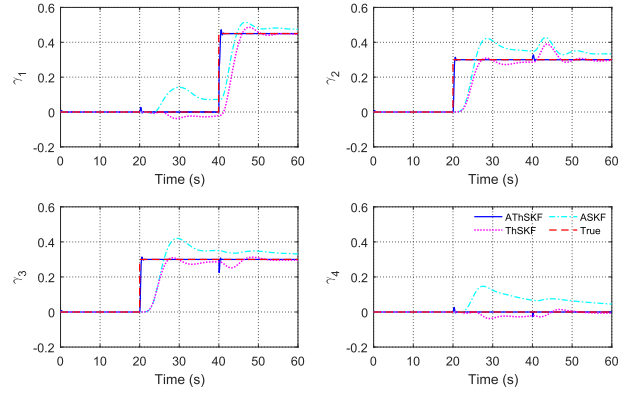


FIGURE 10. Fault estimation performance of ASKF, ThSKF and ATsKF in scenario 3.

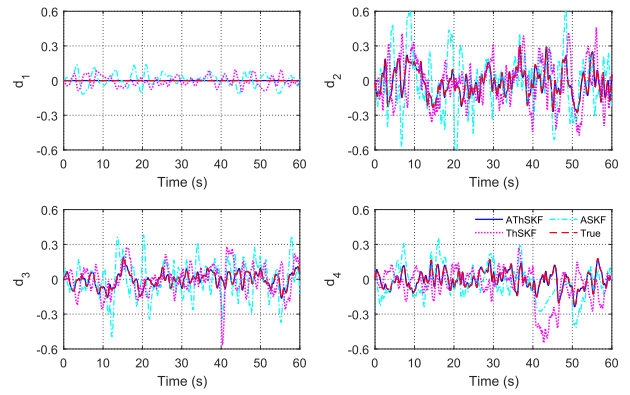


FIGURE 11. Disturbance estimation performance of ASKF, ThSKF and ATsKF in scenario 3.

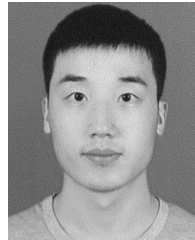
rendered in the motors. For instance, the estimate value of height z achieved by ASKF and ThSKF deviates largely from the true value during $20s < t < 60s$. From Fig. 10, one can see that the fault estimate using ATsKF is better than that using ASKF and ThSKF. The occurrence of simultaneous actuator faults has no effect on the fault estimation performance of ATsKF, but the estimation of actuator faults using ASKF and ThSKF degrades. Fig. 11 illustrates the disturbance estimation performance of ATsKF in scenario 3, which is as good as in Fig. 8.

V. CONCLUSIONS

In this paper, a robust FDD scheme is proposed to estimate actuator faults for QUAV with the influence of external disturbances. An adaptive three-state Kalman filter is designed by decoupling an adaptive augmented state Kalman filter into three parallel sub-filters. The ATsKF-based FDD scheme can detect and estimate actuator faults even when the dynamic model of actuator faults and external disturbances are not perfectly known. The estimates of actuator faults and external disturbances will be conducive to improving the system performance. The simulation results demonstrate the proposed FDD scheme have not only a satisfactory state performance, but also an acceptable fault performance. In future work, The ATsKF-based FDD scheme will be integrated with fault-tolerant control system.

REFERENCES

- [1] A. C. Satici, H. Poonawala, and M. W. Spong, "Robust optimal control of quadrotor UAVs," *IEEE Access*, vol. 1, pp. 79–93, 2013.
- [2] K. Alexis, G. Nikolakopoulos, A. Tzes, and L. Dritsas, "Coordination of helicopter UAVs for aerial forest-fire surveillance," in *Applications of Intelligent Control to Engineering Systems*, vol. 39. Dordrecht, The Netherlands: Springer, 2009, pp. 169–193.
- [3] L. F. Luque-Vega, B. Castillo-Toledo, A. Loukianov, and L. E. Gonzalez-Jimenez, "Power line inspection via an unmanned aerial system based on the quadrotor helicopter," in *Proc. IEEE 17th Medit. Electrotech. Conf.*, Apr. 2014, pp. 393–397.
- [4] Y. M. Zhang et al., "Development of advanced FDD and FTC techniques with application to an unmanned quadrotor helicopter testbed," *J. Franklin Inst.*, vol. 350, no. 9, pp. 2396–2422, 2013.
- [5] Z. Liu, C. Yuan, X. Yu, and Y. Zhang, "Retrofit fault-tolerant tracking control design of an unmanned quadrotor helicopter considering actuator dynamics," *Int. J. Robust Nonlinear Control*, vol. 24, 2017, doi: [10.1002/rnc.3889](https://doi.org/10.1002/rnc.3889).
- [6] S. A. Raza, "Autonomous UAV control for low-altitude flight in an urban gust environment," Ph.D. dissertation, Dept. Mech. Aerosp. Eng., Carleton Univ., Ottawa, ON, Canada, 2015.
- [7] Y. Zhang and J. Jiang, "Bibliographical review on reconfigurable fault-tolerant control systems," *Annu. Rev. Control*, vol. 32, no. 2, pp. 229–252, 2008.
- [8] Y. M. Zhang and J. Jiang, "Active fault-tolerant control system against partial actuator failures," *IEE Proc.–Control Theory Appl.*, vol. 149, no. 1, pp. 95–104, Jan. 2002.
- [9] M. H. Amoozgar, A. Chamseddine, and Y. Zhang, "Experimental test of a two-stage Kalman filter for actuator fault detection and diagnosis of an unmanned quadrotor helicopter," *J. Intell. Robot. Syst.*, vol. 70, pp. 107–117, Apr. 2013.
- [10] R. C. Avram, X. Zhang, and J. Muse, "Quadrotor actuator fault diagnosis and accommodation using nonlinear adaptive estimators," *IEEE Trans. Control Syst. Technol.*, vol. 25, no. 6, pp. 2219–2226, Nov. 2017.
- [11] Z. Cen, H. Noura, B. T. Susilo, and Y. A. Younes, "Robust fault diagnosis for quadrotor UAVs using adaptive Thau observer," *J. Intell. Robot. Syst.*, vol. 73, nos. 1–4, pp. 573–588, Jan. 2014.
- [12] W. Han, Z. Wang, and S. Yi, "Fault estimation for a quadrotor unmanned aerial vehicle by integrating the parity space approach with recursive least squares," *Proc. Inst. Mech. Eng. G, J. Aerosp. Eng.*, vol. 232, no. 4, pp. 783–796, 2018.
- [13] Y. Wang, B. Jiang, N. Lu, and J. Pan, "Hybrid modeling based double-granularity fault detection and diagnosis for quadrotor helicopter," *Nonlinear Anal., Hybrid Syst.*, vol. 21, pp. 22–36, Aug. 2016.
- [14] J. Chen and R. J. Patton, "Optimal filtering and robust fault diagnosis of stochastic systems with unknown disturbances," *IEE Proc.–Control Theory Appl.*, vol. 143, no. 1, pp. 31–36, Jan. 1996.
- [15] S. Shao, M. Chen, and X. Yan, "Adaptive sliding mode synchronization for a class of fractional-order chaotic systems with disturbance," *Nonlinear Dyn.*, vol. 83, no. 4, pp. 1855–1866, 2016.
- [16] F. Liu, J. Huang, Y. Shi, and D. Xu, "Fault detection for discrete-time systems with randomly occurring nonlinearity and data missing: A quadrotor vehicle example," *J. Franklin Inst.*, vol. 350, pp. 2474–2493, Nov. 2013.
- [17] M. Frangenberg, J. Stephan, and W. Fichter, "Fast actuator fault detection and reconfiguration for multicopters," in *Proc. AIAA Guid., Navigat., Control Conf.*, 2015, pp. 1766–1790.
- [18] Y. Yi and Y. Zhang, "Fault diagnosis of an unmanned quadrotor helicopter based on particle filter," in *Proc. Int. Conf. Unmanned Aircr. Syst. (ICUAS)*, Jun. 2017, pp. 1432–1437.
- [19] K. Alexis, G. Nikolakopoulos, and A. Tzes, "Switching model predictive attitude control for a quadrotor helicopter subject to atmospheric disturbances," *Control Eng. Pract.*, vol. 19, no. 10, pp. 1195–1207, Oct. 2011.
- [20] D. Shi, Z. Wu, and W. Chou, "Generalized extended state observer based high precision attitude control of quadrotor vehicles subject to wind disturbance," *IEEE Access*, May 2018, pp. 32349–32359, doi: [10.1109/ACCESS.2018.2842198](https://doi.org/10.1109/ACCESS.2018.2842198).
- [21] L. Besnard, Y. B. Shtessel, and B. Landrum, "Quadrotor vehicle control via sliding mode controller driven by sliding mode disturbance observer," *J. Franklin Inst.*, vol. 349, no. 2, pp. 658–684, 2012.
- [22] F. Chen, F. Lu, B. Jiang, and G. Tao, "Adaptive compensation control of the quadrotor helicopter using quantum information technology and disturbance observer," *J. Franklin Inst.*, vol. 351, pp. 442–455, Jan. 2014.
- [23] S. A. Raza, J. Etele, and G. Fusina, "Hybrid controller for improved position control of quadrotors in urban wind conditions," *J. Aircr.*, vol. 55, no. 3, pp. 1014–1023, 2018.
- [24] P. Lu, "Fault diagnosis and fault-tolerant control for aircraft subjected to sensor and actuator faults," Ph.D. dissertation, Dept. Aerosp. Eng., Delft Univ. Technol., Delft, The Netherlands, 2016.
- [25] N. Meskin, K. Khorasani, and C. A. Rabath, "A hybrid fault detection and isolation strategy for a network of unmanned vehicles in presence of large environmental disturbances," *IEEE Trans. Control Syst. Technol.*, vol. 18, no. 6, pp. 1422–1429, Nov. 2010.
- [26] Y. Zhong, W. Zhang, and Y. Zhang, "Sensor fault diagnosis for unmanned quadrotor helicopter via adaptive two-stage extended Kalman filter," in *Proc. Int. Conf. Sens., Diagnostics, Prognostics, Control*, Aug. 2017, pp. 493–498.
- [27] Y. Guo, B. Jiang, and Y. Zhang, "A novel robust attitude control for quadrotor aircraft subject to actuator faults and wind gusts," *IEEE/CAA J. Autom. Sinica*, vol. 5, no. 1, pp. 292–300, Jan. 2018.
- [28] M. A. Kamel, X. Yu, and Y. M. Zhang, "Fault-tolerant cooperative control design of multiple wheeled mobile robots," *IEEE Trans. Control Syst. Technol.*, vol. 26, no. 2, pp. 756–764, Mar. 2018.
- [29] A. T. Alouani, P. Xia, T. R. Rice, and W. D. Blair, "On the optimality of two-stage state estimation in the presence of random bias," *IEEE Trans. Autom. Control*, vol. 38, no. 8, pp. 1279–1283, Aug. 1993.
- [30] J. Y. Keller and M. Darouach, "Optimal two-stage Kalman filter in the presence of random bias," *Automatica*, vol. 33, pp. 1745–1748, Sep. 1997.
- [31] Q. Xia, M. Rao, Y. Ying, and X. Shen, "Adaptive fading Kalman filter with an application," *Automatica*, vol. 30, no. 8, pp. 1333–1338, 1994.
- [32] K. H. Kim, J. G. Lee, and C. G. Park, "Adaptive two-stage Kalman filter in the presence of unknown random bias," *Int. J. Adapt. Control Signal Process.*, vol. 20, no. 7, pp. 305–319, 2006.
- [33] B. Friedland, "Treatment of bias in recursive filtering," *IEEE Trans. Autom. Control*, vol. 14, no. 4, pp. 359–367, Aug. 1969.
- [34] F. Ben Hmida, K. Khémiri, J. Ragot, and M. Gossa, "Three-stage Kalman filter for state and fault estimation of linear stochastic systems with unknown inputs," *J. Franklin Inst.*, vol. 349, pp. 2369–2388, Sep. 2012.
- [35] Y.-M. Chen, Y.-L. He, and M.-F. Zhou, "Decentralized PID neural network control for a quadrotor helicopter subjected to wind disturbance," *J. Central South Univ.*, vol. 22, pp. 168–179, Jan. 2015.



YUJIANG ZHONG received the M.S. degree from Northwestern Polytechnical University, Xi'an, Shaanxi, China, in 2014, where he is currently pursuing the Ph.D. degree. He is with the Department of Mechanical, Industrial and Aerospace Engineering, Concordia University, Montreal, QC, Canada. His research interests include fault detection and diagnosis, fault-tolerant control, and adaptive control.



YOUNMIN ZHANG (M'99–SM'07) is currently a Professor with the Department of Mechanical, Industrial and Aerospace Engineering, Concordia Institute of Aerospace Design and Innovation, Concordia University, Canada. He has published four books, over 460 journal and conference papers, and book chapters. His main research interests and experience are in the areas of condition monitoring, health management, fault detection and diagnosis, fault-tolerant control systems, and cooperative and fault-tolerant cooperative guidance, navigation, and control. He is a fellow of CSME, a Senior Member of AIAA, and a member of the Technical Committee (TC) for several scientific societies. He has served as the General Chair, the Program Chair, and a IPC Member of many international conferences. He has been invited to deliver plenary talks at international conferences/workshops and research seminars worldwide for over 90 times. He is an Editor-in-Chief of the *Journal of Instrumentation, Automation and Systems*, an Editor-at-Large of the *Journal of Intelligent and Robotic Systems*, and an Editorial Board Member/Associate Editor of several other international journals (including three newly launched journals on unmanned systems). More detailed information can be found at <http://users.encs.concordia.ca/~ymzhang/>.



WEI ZHANG was born in 1963. He received the B.S. and M.S. degrees in flight mechanics and the Ph.D. degree in aircraft design from Northwestern Polytechnical University. He was an Associate Professor with the School of Creative Media, City University of Hong Kong, from 2013 to 2014. He is currently a Professor with the School of Aeronautics, Northwestern Polytechnical University. His research interests include aircraft design methodology, system integration and design, scaled flight testing, and aircraft system identification.



JUNYI ZUO received the B.S. and M.S. degrees from the School of Aeronautics, Northwestern Polytechnical University, in 2000 and 2003, respectively, and the Ph.D. degree from the School of Automation, Northwestern Polytechnical University, in 2008. He is currently an Associate Professor with the School of Aeronautics, Northwestern Polytechnical University. His research interests include optimal estimation theory and its application, nonlinear filtering, target tracking, aircraft system identification.



HAO ZHAN received the B.S., M.S., and Ph.D. degrees from Northwestern Polytechnical University, China, in 1994, 1997, and 2000, respectively. He was a Post-Doctoral Fellow with Beihang University from 2000 to 2002. In 2001, he joined the German Aerospace Center as a Research Associate. From 2003 to 2005, he was a Post-Doctoral Fellow at Northwestern Polytechnical University. He is currently a Professor with the School of Aeronautics, Northwestern Polytechnical University. His research interests include flight dynamic and control, aircraft design, and fluid mechanics.

• • •